The Role of Silver Nanoparticles in Enhancing the Structural and Antibacterial Properties of Chitosan/PEO Blend Films

Asmaa H. Mujalli and Najwa J. Jubier
Department of Physics, Wasit University, College of Science, 52001 Al-Kut, Wasit, Iraq
std2023204.amujalli@uowasit.edu.iq, njassim@uowasit.edu.iq

Keywords: Chitosan, Polyethylene Oxide, Silver Nanoparticles, Nanocomposites, Antibacterial Activity.

Abstract: The current study investigates the enhancement of the structural, morphological, and antibacterial properties of a nanocomposite material composed of chitosan (CS) and polyethylene oxide (PEO). The improvement is achieved through the incorporation of silver nanoparticles (AgNPs) at varying concentrations of 1%, 3%, and 5%. A variety of analytical techniques were applied. The XRD, FE-SEM, and FTIR investigations revealed that the introduction of AgNPs induced substantial alterations in the crystallinity of the material, the characteristics of its surface, and the behavior of functional groups within the polymer matrix. The changes observed in these parameters underscore the influence of AgNPs on the fundamental properties of the CS/PEO blend. To further characterize the nanocomposites, Zeta Potential analysis was performed. This technique provides important information about the stability and surface charge characteristics of the nanocomposites, which in turn allows for a better understanding of the dispersion and distribution of nanoparticles within the polymer matrix. Antibacterial tests demonstrated enhanced inhibition against Staphylococcus aureus and Escherichia coli, particularly in AgNP-containing films. The combined effects of chitosan and AgNPs contributed to strong antibacterial performance, especially against Gram-positive bacteria.

1 INTRODUCTION

Material science benefits greatly from nanotechnology since it allows scientists to alter polymer characteristics for creating new materials. The ratio between surface area and volume makes nanotechnology-based composites both thermally and electrically stable which makes them more efficient at reduced cost [1], [2]. Multiple studies explore nanocomposites that use synthetic polymers combined with metal oxide and carbon filler nanomaterials for enhancing multiple functional properties [3], [4].

Chitosan obtains its nature as a biodegradable biocompatible polymer from chitin through deacetylation. The many functional groups in chitosan strengthen structure while enhancing biological functions which results in its efficient antimicrobial properties. The medical sector frequently employs chitosan as an effective material because this compound achieves low toxicity alongside its capability to develop films and hydrogels and nanoparticles [5]-[10].

The properties of chitosan nanoparticles (CNPs) become more useful for biomedical and environmental applications because they show improved biocompatibility together with antimicrobial activity and membrane penetration capabilities [11]-[13]. PEO features versatility as a stretchable non-toxic substance because it dissolves well in water through hydrogen bond interactions that unite with chitosan into a single homogeneous material that demonstrates better physicochemical behavior. PEO demonstrates ideal properties for medical uses because it matches human tissue composition so it finds applications in wound dressing and drug delivery systems [5], [14]. The casting method functions as a common approach to develop nanocomposite systems which exhibit improved structural and optical properties [15]. Nanotechnology integration into polymers resulted in the development of nanocomposites that boost biomedical materials' properties and support complex medical applications [16]. The materials achieve outstanding properties regarding mechanical performance combined with strength and durability alongside wear resistance characteristics thus providing high effectiveness for medical implementations and engineering applications [2], [17] and [18]. Additionally, several polymer blends have shown antibacterial potential when reinforced with metal oxide or silver nanoparticles [19]. Among

nanomaterials, metallic nanoparticles (1-100 nm) possess unique physical and chemical properties, such as high catalytic activity, making them valuable in research on microbial resistance to antibiotics [20], [21]. Silver, copper, and zinc are commonly used as antimicrobial agents, with studies showing that silver nanoparticles (AgNPs) demonstrate the highest effectiveness against Streptococcus mutans [22]. Additionally, AgNPs exhibit strong antimicrobial activity against bacteria, fungi, and viruses, renewing interest in their medical applications, particularly against resistant strains [23].

This study investigates the structural and antibacterial properties of chitosan/PEO nanocomposite films reinforced with silver nanoparticles. XRD, FE-SEM, AFM, FTIR, EDX, zeta potential analysis, and antibacterial testing were employed to assess the impact of AgNP concentration to emphasize their potential for biomedical applications.

2 EXPERIMENTAL WORK

2.1 Materials

Chitosan (≥90% purity, 30–50 nm) was obtained from Nanochemazone, Polyethylene oxide (PEO) (Mw = 3,000,000 g/mol, ≥98% purity) was purchased from Cheng Du Micxy Chemical Co., Ltd., and silver nanoparticles (AgNPs) (10–20 nm, ≥99.9% purity) were supplied by Sky Spring Nanomaterials. Acetic acid (≥99.7% purity) was used as a solvent and deionized distilled water to ensure the purity of the sample.

AFM test was conducted to analyze the initial surface morphology and roughness of the raw materials, which include chitosan, polyethylene oxide (PEO), and silver nanoparticles (AgNPs). Measurements were performed at a scan size of 2.0 × 0.2 µm. Table 1 indicates that the PEO powder demonstrated the greatest surface roughness (Rq = 25.72 nm), signifying a markedly uneven structure. Conversely, chitosan powder exhibited a more uniform shape (Rq = 19.91 nm). AgNPs demonstrated the lowest Rq value (12.78 nm), indicating their nanometric scale and reasonably uniform distribution, as illustrated in Figure 1. The average particle sizes determined via AFM line analysis were 48.18 nm for chitosan, 78.88 nm for PEO and 38.87 nm for AgNPs, thereby affirming the nanoscale characteristics of the materials.

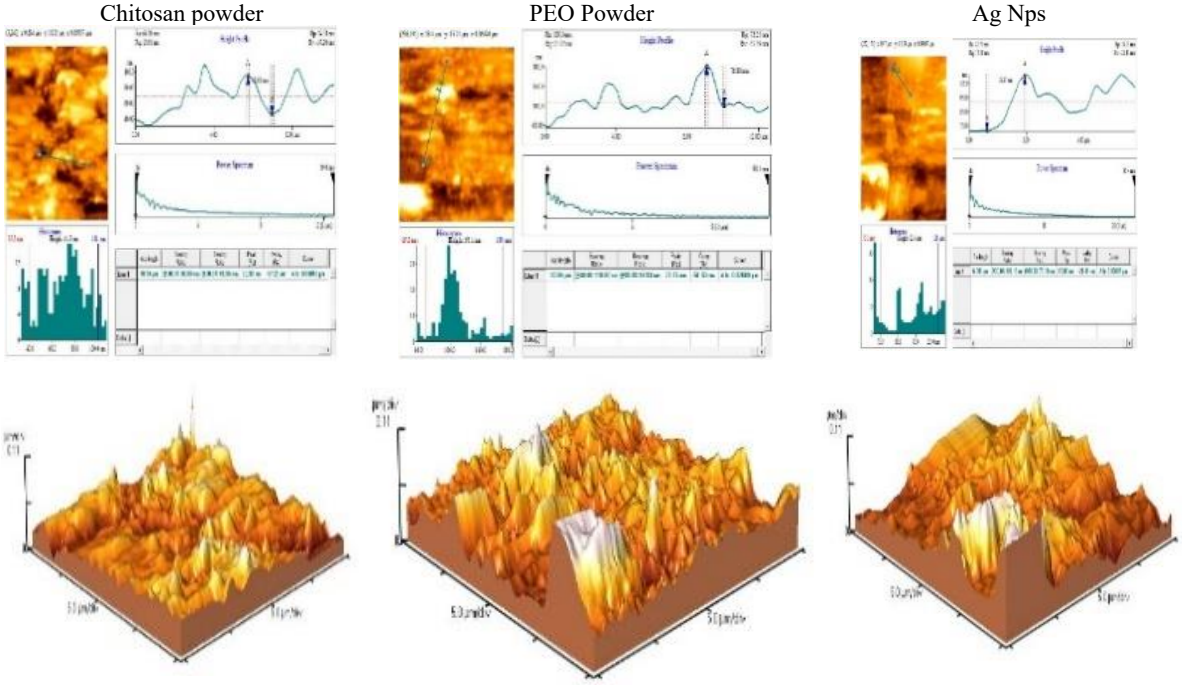

Figure 1: AFM images of chitosan, PEO, and AgNPs powders at 2.0 µm/div magnification.

Table 1. AFM roughness parameters and average particle sizes of raw materials:

Sample	Rq (nm)	Rp (nm)	Rv (nm)	Max Height (nm)	Average Particle Size (nm)
Chitosan	19.91	39.38	-37.20	61.3	48.18
PEO	25.72	72.25	-51.59	99.1	78.88
AgNPs	12.78	19.03	-21.41	32.4	38.87

2.2 Methods of Preparation

The chitosan/polyethylene oxide (Cs/PEO) composite augmented with silver nanoparticles (AgNPs) was synthesized via the solution casting technique. One gram of chitosan was dissolved in 100 milliliters of 1% acetic acid and agitated at 300 revolutions per minute for six hours at ambient temperature. PEO (1 g) was independently dissolved in 100 mL of distilled water at 50°C. The PEO solution was incrementally incorporated into the chitosan solution while maintaining continuous agitation until a uniform mixture was achieved. Silver nanoparticles (AgNPs) were integrated at concentrations of 1%, 3%, and 5%, thereafter subjected to ultrasonic treatment (120 W, 1 hour) to guarantee uniform dispersion. The finished solution was deposited into 14 cm Petri plates and desiccated at ambient temperature for 5 days; the preparation methods are illustrated in Figure 2.

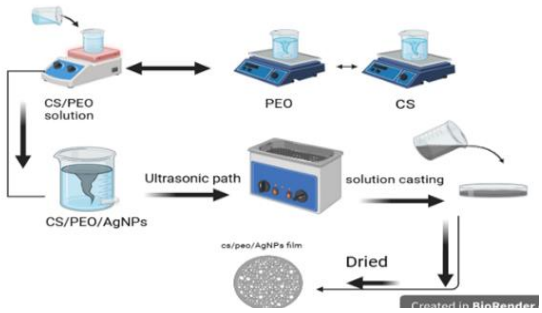

Figure 2: Schematic representation of the preparation process of chitosan/PEO/AgNPs nanocomposite films.

2.2.1 Characterization Techniques

Structural, and morphological, properties were analyzed using multiple techniques such as XRD (Philips XPERT-PRO) to determine crystallinity and phase composition (Cu-Kα, 10°–80°), EDX confirmed elemental composition, and the presence of AgNPs, FTIR (Shimadzu IR Affinity) was used to identify functional groups in the range of 4000–400 cm^{-1}, Zeta Potential measurements (Horiba SZ-100) were conducted to evaluate the surface charge and colloidal stability at 25°C, The agar disk diffusion was used to identify the antibacterial activity against S. aureus and E. coli. The tested sample was loaded on the well, and bacterial cultures were placed on Mueller-Hinton agar plate. Measurement of inhibition zones was done after a 24 hours incubation at 37 o C. Distilled as the negative control water was used.

3 RESULTS AND DISCUSSION

3.1 XRD Analysis

Figure 3 displays the XRD patterns of chitosan (Cs) (S1), polyethylene oxide (PEO) (S2), Cs/PEO mix (S3), and Cs/PEO combined with varying concentrations (1, 3, 5) % of silver nanoparticles (AgNPs) (S4, S5, S6) accordingly. The diffraction peaks at 2θ = 10.5° and 20.1° signify an orthorhombic structure, with supplementary peaks corroborating the semi crystalline characteristics of chitosan [24]-[26]. In contrast, PEO had specific peaks at 2θ = 19.2°, 21.0°, 23.3°, and 26.3°, signifying its monoclinic crystalline structure, accompanied by smaller peaks at 27.1° [27]. The XRD pattern of the Cs/PEO blend exhibited peaks from both constituents, hence affirming effective synthesis. The peak at 2θ = 23.1°, linked to PEO, diminished in intensity and widened, signifying hydrogen bonding interactions between Cs and PEO [28]. The crystallite size (D) for the (111) peak was determined using the Debye-Scherrer equation [29] ($D=K\lambda/\beta \cos\theta$), where K is a constant (0.91), λ represents the X-ray wavelength (0.154 nm), β denotes the full width at half maximum (FWHM), and θ signifies the diffraction angle. The mean crystallite size of AgNPs rose from 15.8 nm (S4) to 21.6 nm (S5) and 25.7 nm (S6), signifying improved crystallization with increased AgNP concentrations, and a decrease in FWHM from 0.52° to 0.32°. The peak at 2θ = 32.004° indicates potential surface crystallization on AgNPs resulting from polymer-nanoparticle interactions, a process documented in prior nanocomposite research [30].

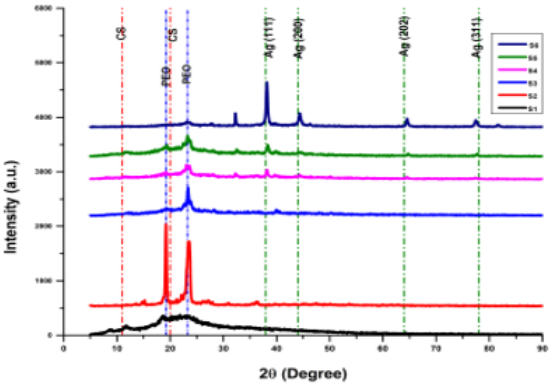

Figure 3: XRD patterns of all samples, including pure chitosan, pure PEO, chitosan/PEO blend, and chitosan/PEO blend with 1%, 3%, and 5% AgNPS.

3.2 FTIR Analysis

Figure 4 presents the FTIR spectra of chitosan (Cs), PEO, their blend (Cs/PEO), and Cs/PEO reinforced with different AgNP concentrations.

In the chitosan spectrum, a broad peak at 3360–3285 cm^{-1} corresponds to –OH and –NH stretching vibrations, indicating strong hydrogen bonding. Peaks at 1645 cm^{-1} (C=O) and 1534 cm^{-1} (N–H) confirm the presence of amide structures [25], [31].

The PEO spectrum exhibits a strong absorption peak at 1094 cm^{-1}, attributed to C–O–C ether stretching, along with weak absorptions around 2872 cm^{-1}, corresponding to C–H stretching vibrations, characteristic of PEO [26]. In the Cs/PEO blend, a slight shift and intensity reduction of the 3360–3285 cm^{-1} band indicates hydrogen bond formation between chitosan and PEO. Additionally, peaks at 1645.95 cm^{-1} (NH) and 1119.48 cm^{-1} (C–O–C) confirm structural interactions within the blend [1].

Upon silver incorporation (S3–S6), spectral changes were observed, particularly in the 4000–1000 cm^{-1} range. While the 4000–3000 cm^{-1} region remained stable, the 3000–1500 cm^{-1} range showed variations in C–H (2900 cm^{-1}) and C=O (1650 cm^{-1}) peaks, indicating silver interactions. The most significant changes occurred in the fingerprint region (1500–1000 cm^{-1}), where increased silver content enhanced C–O (1000–1200 cm^{-1}) intensity, suggesting direct interactions with oxygen-containing groups. The results suggest that silver modifies the molecular structure by interacting with oxygen-containing groups while maintaining the composite's fundamental structure, consistent with previous studies like Mahmoud et al. (2019) [19], [32].

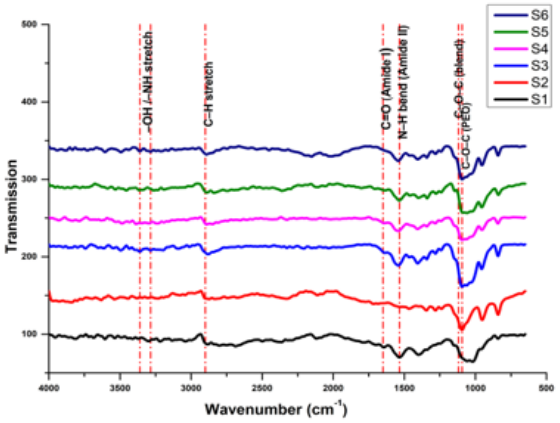

Figure 4: FTIR spectra of all samples, including pure chitosan, pure PEO, chitosan/PEO blend, and chitosan/PEO blend with 1%, 3%, and 5% AgNPS, showing the characteristic functional groups and interactions.

3.3 Energy Dispersive X-Ray Spectroscopy (EDX) Results

The elemental composition of the polymeric samples was analyzed using energy-dispersive X-ray Spectroscopy (EDX) to identify the presence of key elements and confirm the structural integrity of the prepared composites.

The EDX spectrum of S1 (Fig. 5), representing pure chitosan, confirmed its organic nature as it primarily consists of carbon (C) and oxygen (O). This composition aligns with the well-documented molecular structure of chitosan, which mainly consists of polysaccharide chains containing carbon, oxygen, and nitrogen [33].

In addition, trace amounts of aluminum (Al) and silicon (Si) were detected, likely originating from the natural mineral content in crustacean shells used as raw material. Previous studies have reported the persistence of these elements despite the demineralization steps during preparation [34].

In sample S3 Figure 6, characterized by an equal mixture of chitosan and PEO, EDX analysis indicated elevated concentrations of carbon (56.17%) and oxygen (38.80%), underscoring the organic composition of the polymeric structure. Nitrogen is derived from chitosan, whereas the oxygen concentration is indicative of both components' contributions. A minimal quantity of chlorine was also identified, presumably due to the processing procedure. The results demonstrate the effective amalgamation of both polymers and the establishment of a stable composite structure.

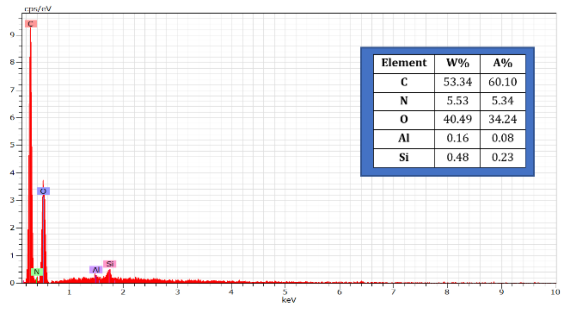

Element	W%	A%
C	53.34	60.10
N	5.53	5.34
O	40.49	34.24
Al	0.16	0.08
Si	0.48	0.23

Figure 5: EDX spectrum and elemental composition of S1 (Cs).

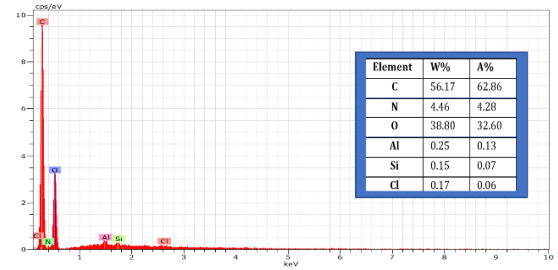

Element	W%	A%
C	56.17	62.86
N	4.46	4.28
O	38.80	32.60
Al	0.25	0.13
Si	0.15	0.07
Cl	0.17	0.06

Figure 6: EDX spectrum and elemental composition of S3 (chitosan/PEO blend).

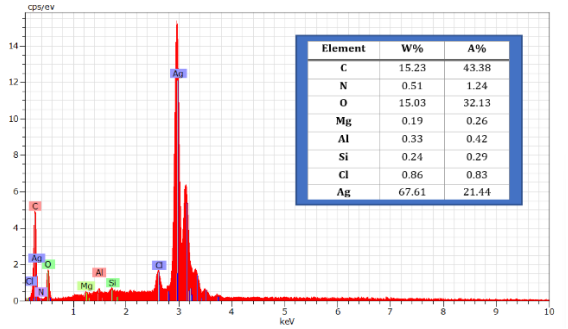

Element	W%	A%
C	15.23	43.38
N	0.51	1.24
O	15.03	32.13
Mg	0.19	0.26
Al	0.33	0.42
Si	0.24	0.29
Cl	0.86	0.83
Ag	67.61	21.44

Figure 7: EDX spectrum and elemental composition of S6 (chitosan/PEO blend with 5% AgNP.

EDX analysis of sample S6 Figure 7 confirmed the presence of silver at 7.52 wt%, indicating the successful incorporation of silver nanoparticles into the polymer matrix. The carbon and oxygen contents remained stable, suggesting that the polymer structure was not significantly affected. The nitrogen content (3.96%) was within the expected range.

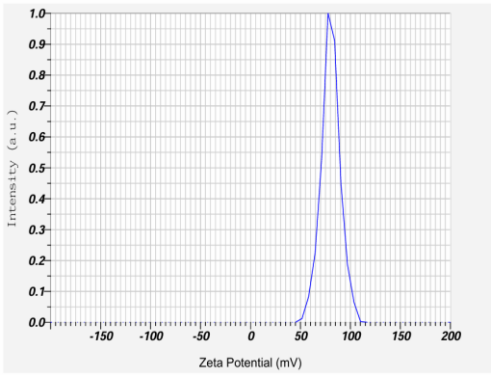

S1

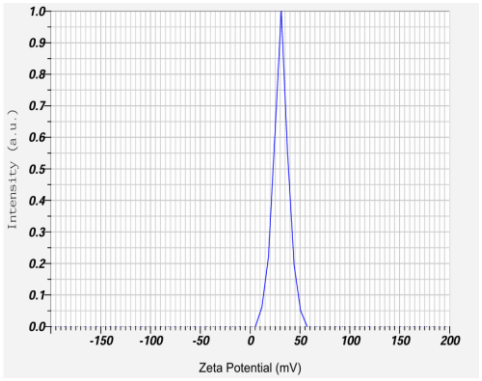

S2

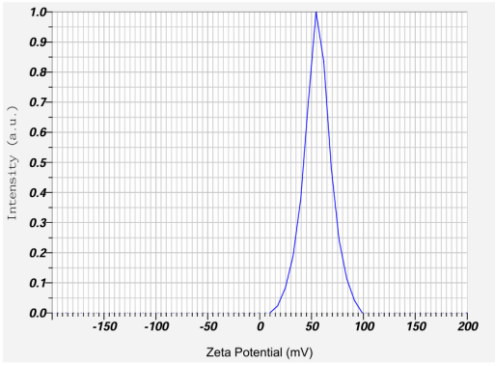

S3

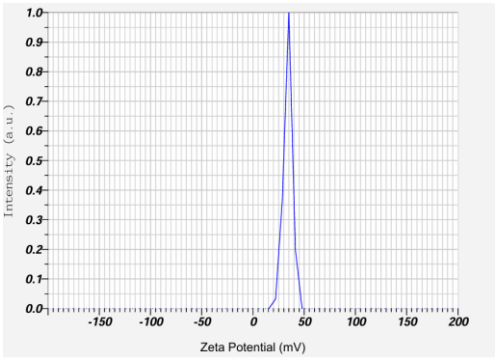

S6

Figure 8: Zeta potential curves of the selected samples (S1, S2, S3, and S6).

3.4 Zeta Potential Analysis

The surface charge of the prepared films was evaluated using Zeta Potential measurements at 25 °C using a Horiba SZ-100 as in Table 2 and Figure 8.

The chitosan membrane (S1) exhibited a high positive Zeta Potential of 80.2 mV, attributed to the protonation of amino groups, indicating excellent stability in acidic environments [35]. In contrast, the PEO film (S2) showed a significantly lower value (30.8 mV), consistent with its neutral chemical nature and known tendency to screen surface charges, thereby reducing electrostatic interactions [36].

Table 2: Zeta Potential values of the selected membrane samples.

Samples	Zeta Potential (Mv)
S1	80.2
S2	30.8
S3	55.7
S6	34.0

The CS/PEO blend (S3) showed an intermediate value (55.7 mV), suggesting enhanced intermolecular interaction and partial retention of chitosan's surface charge. This can be attributed to hydrogen bonding between –NH and –OH groups of chitosan and the ether oxygen in PEO [28].The nanocomposite film containing 5% AgNPs (S6) exhibited a reduced Zeta Potential (34.0 mV), which may be attributed to nanoparticle agglomeration or surface charge masking by the polymer matrix. This observation agrees with previous reports suggesting that at higher AgNP concentrations, particles tend to aggregate, reducing the active surface area and weakening electrostatic interactions [37], [38].

Despite the lower surface charge, it is reported that chitosan-AgNPs systems can retain some positive charge due to protonated amino groups, which contributes to their antibacterial potential [39].

3.5 Antibacterial Activity Analysis

The antibacterial properties of the chitosan/PEO-AgNPs solution were evaluated using the agar well diffusion method, showing a concentration-dependent effect. According to Table 3, inhibition zones ranged from 6.5 mm (lowest concentration) to 26 mm (highest concentration), confirming their effectiveness.

When tested against Staphylococcus aureus, S6 exhibited the highest antibacterial activity, with an inhibition zone of 26 mm at 100% concentration, consistent with previous findings reporting that Cs/Ag NPs maintain strong antibacterial effects even at low concentrations [40]. S3, S4, and S5 also showed inhibition zones exceeding 23 mm, reinforcing the bactericidal effect of silver incorporation Figure 9.

Table 3: Antibacterial activity of chitosan/PEO nanocomposite solution against Staphylococcus aureus (Gram-positive) and Escherichia coli (Gram-negative) bacteria, represented by the inhibition zone (mm) at different concentrations.

Samples		A control	B 12.5%	C 25%	D 50%	E 100%
S.aures	S 1	6	6.5	11	14.5	19
	S 2	6	8.6	12.7	14	17
	S 3	6	8	9	20.9	23.7
	S 4	6	7	12	19.5	24
	S 5	6	11	16	21	23
	S 6	6	8.5	10	20	26
E. coli	S 1	6	9	12	14	18
	S 2	6	11	12	13	17
	S 3	6	10.5	14	15	18
	S 4	6	8	13	17	20
	S 5	6	9	9.5	16	22
	S 6	6	8	11	17	21

Against Escherichia coli, antibacterial efficacy was lower, with S5 showing the highest inhibition zone (22 mm at 100%), likely due to the outer membrane barrier of Gram-negative bacteria, which limits nanoparticle penetration, as previously reported Figure 10 [41], [42].

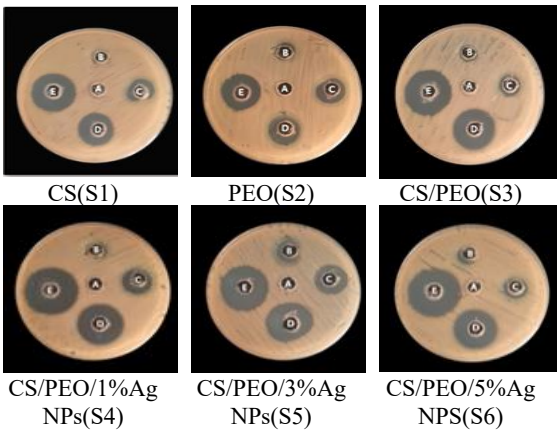

Figure 9: Antibacterial activity of chitosan, PEO, and chitosan/PEO nanocomposite films with different silver nanoparticle concentrations against Gram-positive Staphylococcus aureus bacteria, showing the inhibition zones for each sample.

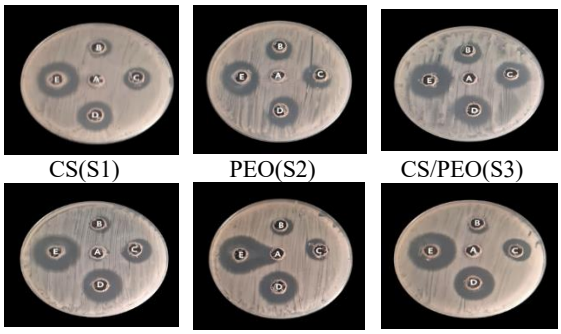

Figure 10: Antibacterial activity of chitosan, PEO, and chitosan/PEO nanocomposite films with different silver nanoparticle concentrations against Gram-negative Escherichia coli bacteria, showing the inhibition zones for each sample.

The observed antibacterial properties a direct correlation was observed between silver concentration and inhibition zone size, with increased silver content enhancing bacterial inhibition, as confirmed by previous studies reporting that higher silver content promotes antimicrobial ion release [40], [41].

The potential of silver-based nanocomposites has been confirmed, particularly against Gram-positive bacteria, while further modifications are still required to improve their efficacy against E. coli. The importance of continued research on long-term stability and interactions in medical applications has also been highlighted in previous studies [40], [43].

4 CONCLUSIONS

Incorporating silver nanoparticles (AgNPs) into the chitosan/PEO composite improved their structural integrity and antibacterial efficacy. XRD analysis confirmed the semi-crystalline nature of the blend and verified AgNPs incorporation through distinct diffraction peaks, including those corresponding to silver, while EDX verified silver presence and increasing Ag content with concentration. FTIR revealed strong chitosan-PEO hydrogen bonding, with spectral shifts indicating AgNP-polymer interactions. With spectral shifts indicating chemical interactions between AgNPs and polymer. Zeta potential analysis demonstrated significant variations in surface charge, reflecting changes in colloidal stability and electrostatic interactions due to AgNPs addition, where Antibacterial activity shows improved inhibition zones against Staphylococcus aureus and E. coli, with stronger effects on Gram-positive bacteria, confirming the synergistic antimicrobial effect of chitosan and AgNPs. The antibacterial response depended on both concentration and strain. S6 (5% AgNPs) demonstrated the most potent suppression of Staphylococcus aureus, while S5 (3% AgNPs) exhibited the greatest antibacterial efficacy against Escherichia coli. The results indicate that AgNP-reinforced CS/PEO composites are viable options for biomedical applications, including antimicrobial wound dressings. Future investigations must prioritize the assessment of long-term stability, cytotoxicity, and in vivo biocompatibility for clinical application.

ACKNOWLEDGMENTS

We would like to thank the University of Wasit, College of Science, Department of Physics, for providing the facilities and technical support essential to this research.

REFERENCES

[1] H. Yunus, “Characterization and antibacterial activity of electrospun polyethylene oxide/chitosan nanofibers,” Tekstil ve Konfeksiyon, vol. 33, no. 1, 2023.

[2] A. Musa, A. Bello, M. A. Sani, A. P. Onwualu, V. O. Anye, and K. A. Bello, et al., “Nano-enhanced polymer composite materials: A review of current advancements and challenges,” Preprints, 2024.

[3] H. S. Mahmood and N. F. Habubi, “Structural, mechanical and magnetic properties of PVA-PVP: Iron oxide nanocomposite,” Appl. Phys. A, vol. 128, p. 956, 2022.

[4] H. S. Mahmood and N. F. Habubi, “Physical properties of PVA: PVP blend reinforced by MWCNT,” J. Phys. Conf. Ser., vol. 2322, p. 012068, 2022.

[5] L. Murillo, P. J. Rivero, X. Sandúa, G. Pérez, J. F. Palacio, and R. J. Rodríguez, “Antifungal activity of chitosan/poly(ethylene oxide) blend electrospun polymeric fiber mat doped with metallic silver nanoparticles,” Polymers, vol. 15, no. 18, Sep. 2023.

[6] M. Chandrasekaran, K. D. Kim, and S. C. Chun, “Antibacterial activity of chitosan nanoparticles: A review,” Processes, vol. 8, 2020.

[7] G. P. Tamilarasi, G. Sabarees, K. Manikandan, S. Gouthaman, V. Alagarsamy, and V. R. Solomon, “Advances in electrospun chitosan nanofiber biomaterials for biomedical applications,” Mater. Adv., vol. 4, pp. 3114-3139, 2023.

[8] M. M. Islam, M. Shahruzzaman, S. Biswas, M. Nurus Sakib, and T. U. Rashid, “Chitosan based bioactive materials in tissue engineering applications-A review,” Bioact. Mater., vol. 5, pp. 164-183, 2020.

[9] M. Supernak, B. Makurat-Kasprolewicz, B. Kaczmarek-Szczepańska, A. Pałubicka, M. Sakowicz-Burkiewicz, and A. Ronowska, et al., "Chitosan-based membranes as gentamicin carriers for biomedical applications-influence of chitosan molecular weight," Membranes, vol. 13, no. 6, Jun. 2023.

[10] F. Bader Hadi, "Characterization of chitosan blends reinforced with nanoparticles for antibacterial applications," Republic of Iraq Ministry of Higher Education.

[11] N. E. A. El-Naggar, S. I. Bashir, N. H. Rabei, and W. E. I. A. Saber, "Innovative biosynthesis, artificial intelligence-based optimization, and characterization of chitosan nanoparticles by Streptomyces microflavus and their inhibitory potential against Pectobacterium carotovorum," Sci. Rep., vol. 12, no. 1, Dec. 2022.

[12] S. Varnaitė-Žuravliova, N. Savest, J. Baltušnikaitė-Guzaitienė, A. Abraitienė, and A. Krumme, "The investigation of the production of salt-added polyethylene oxide/chitosan nanofibers," Materials, vol. 17, no. 1, Jan. 2024.

[13] N. E. A. El-Naggar, S. R. Dalal, A. M. Zweil, and M. Eltarahony, "Artificial intelligence-based optimization for chitosan nanoparticles biosynthesis, characterization and in vitro assessment of its anti-biofilm potentiality," Sci. Rep., vol. 13, no. 1, Dec. 2023.

[14] R. Cuana, T. I. Nasution, H. Agusnar, A. Susilowati, N. S. Lubis, and I. S. Pradana, "Humidity detection based on chitosan/PEO film sensor," in J. Phys. Conf. Ser., 2023.

[15] H. S. Mahmood and N. F. Habubi, "Preparation of samarium doped-PMMA composite by casting method to evaluate the optical properties and potential applications," J. Optoelectron. Adv. Mater., vol. 25, no. 1-2, pp. 56-61, 2023.

[16] Z. Yu, "The application of nanomaterials in medicine," in Highlights in Science, Engineering and Technology MSMEE, vol. 2024, 2024.

[17] M. M. Abutalib and A. Rajeh, "Enhanced structural, electrical, mechanical properties and antibacterial activity of Cs/PEO doped mixed nanoparticles (Ag/TiO_2) for food packaging applications," Polym. Test., vol. 93, Jan. 2021.

[18] H. S. Mahmood and N. F. Habubi, "Mechanical and antibacterial activity of biodegradable Na-CMC: PVA reinforced with Al_2O_3 nanoparticles," Int. J. Nano Biomater., vol. 10, no. 4, pp. 221-234, 2024.

[19] H. S. Mahmood and M. K. Jawad, "Investigation of chitosan/PEO reinforced with AgNPs for antibacterial activity prepared by solution casting method," Ann. Trop. Med. Public Health, vol. 22, no. 9, pp. 70-82, 2019.

[20] P. Sartori, A. P. L. Delamare, G. Machado, D. M. Devine, J. S. Crespo, and M. Giovanela, "Synthesis and characterization of silver nanoparticles for the preparation of chitosan pellets and their application in industrial wastewater disinfection," vol. 15, no. 1, Jan. 2023.

[21] S. Anees Ahmad, S. Sachi Das, A. Khatoon, M. Tahir Ansari, M. Afzal, and M. Saquib Hasnain, et al., "Bactericidal activity of silver nanoparticles: A mechanistic review," Mater. Sci. Energy Technol., vol. 3, pp. 756-769, 2020.

[22] S. Liao, Y. Zhang, X. Pan, F. Zhu, C. Jiang, and Q. Liu, et al., "Antibacterial activity and mechanism of silver nanoparticles against multidrug-resistant Pseudomonas aeruginosa," Int. J. Nanomed., vol. 14, pp. 1469-1487, 2019.

[23] C. G. A. Das, V. G. Kumar, T. S. Dhas, V. Karthick, K. Govindaraju, and J. M. Joselin, et al., "Antibacterial activity of silver nanoparticles (biosynthesis): A short review on recent advances," Biocatal. Agric. Biotechnol., vol. 27, 2020.

[24] R. S. C. M. D. Q. Antonino, B. R. P. L. Fook, V. A. D. O. Lima, R. Í. D. F. Rached, E. P. N. Lima, and R. J. D. S. Lima, et al., "Preparation and characterization of chitosan obtained from shells of shrimp (Litopenaeus vannamei Boone)," Mar. Drugs, vol. 15, no. 5, May 2017.

[25] P. P. Dhawade and R. N. Jagtap, "Characterization of the glass transition temperature of chitosan and its oligomers by temperature modulated differential scanning calorimetry."

[26] N. G. Madian, B. A. El-Ashmanty, and H. K. Abdel-Rahim, "Improvement of chitosan films properties by blending with cellulose, honey and curcumin," Polymers, vol. 15, no. 12, Jun. 2023.

[27] S. Elashmawi, A. A. Al-Muntaser, and A. M. Ismail, "Structural, optical, and dielectric modulus properties of PEO/PVA blend filled with metakaolin," Opt. Mater., vol. 126, p. 112220, Apr. 2022.

[28] N. Al-Harbi, "Preparation and characterization of chitosan/polyethylene oxide nanocomposite films with different concentrations of zirconia nanocomposites," Polym. Test., vol. 128, Nov. 2023.

[29] Challoob, Abdizadeh and N. J. Jubier, "Green synthesis of Ag-Cu NPs using black eggplant extract as the reducing and stabilizing agents: Characterization and energy band gap," in J. Phys. Conf. Ser., vol. 2974, no. 1, p. 012032, Mar. 2025.

[30] G. Vanti, N. Poondla, P. Manogaran, N. Teradal, S. V, and R. Kaulgud, et al., "Synthesis and characterization of multifunctional chitosan-silver nanoparticles: An in-vitro approach for biomedical applications," Pharmaceuticals, vol. 17, no. 9, Sep. 2024.

[31] M. P. M. Hanif, A. J. Jalilah, M. F. H. Anisah, and A. Tilagavathy, "Chitosan/polyethylene oxide (PEO) filled carbonized wood fiber conductive composite film," in Mater. Sci. Forum, pp. 638-644, 2020.

[32] G. A. Mahmoud and D. E. Hegazy, "Radiation synthesis and characterization of polyethylene oxide/chitosan-silver nanocomposite for biomedical applications," Arab J. Nucl. Sci. Appl., vol. 47, 2014.

[33] M. Rinaudo, "Chitin and chitosan: Properties and applications," Prog. Polym. Sci., vol. 31, no. 7, pp. 603-632, 2006.

[34] H. E. Ghannam, A. S. Talab, N. V. Dolganova, A. M. S. Hussein, and N. M. Abdelmaguid, "Characterization of chitosan extracted from different crustacean shell wastes," J. Appl. Sci., vol. 16, no. 10, pp. 454-461, 2016.

[35] N. Saïed and M. Aider, "Zeta potential and turbidimetry analyzes for the evaluation of chitosan/phytic acid complex formation," J. Food Res., vol. 3, no. 2, p. 71, Feb. 2014.

[36] R. Zimmermann, W. Norde, M. A. C. Stuart, and C. Werner, “Electrokinetic characterization of poly(acrylic acid) and poly(ethylene oxide) brushes in aqueous electrolyte solutions,” Langmuir, vol. 21, no. 11, pp. 5108-5114, May 2005.

[37] H. Duman, F. Eker, E. Akdaşçi, A. M. Witkowska, M. Bechelany, and S. Karav, “Silver nanoparticles: A comprehensive review of synthesis methods and chemical and physical properties,” Nanomaterials, vol. 14, 2024.

[38] S. S. Salem, A. Fouda, A. M. Mahdy, N. M. Fahmy, and E. M. Al-Olayan, “Antibacterial, cytotoxicity and larvicidal activities of biosynthesized silver nanoparticles using Penicillium citrinum,” Bull. Natl. Res. Cent., vol. 43, no. 1, pp. 1-11, 2019.

[39] Ge, M. Li, J. Fan, C. Celia, Y. Xie, and Q. Chang, et al., “Synthesis, characterization, and antibacterial activity of chitosan-chelated silver nanoparticles,” J. Biomater. Sci. Polym. Ed., vol. 35, no. 1, pp. 45-62, Jan. 2024.

[40] M. Shehabeldine, S. S. Salem, O. M. Ali, K. A. Abd-Elsalam, F. M. Elkady, and A. H. Hashem, “Multifunctional silver nanoparticles based on chitosan: Antibacterial, antibiofilm, antifungal, antioxidant, and wound-healing activities,” J. Fungi, vol. 8, no. 6, Jun. 2022.

[41] Kasemets, J. Laanoja, M. Sihtmäe, H. Vija, I. Kurvet, and M. Otsus, et al., “Silver-chitosan nanocomposites for biomedical application: Design, synthesis and antimicrobial efficiency,” 2023, p. 40.

[42] W. K. Salman and N. J. Jubier, “Investigating the antibacterial activity of green-synthesized $CuCO_3O_4$ nanoparticles,” in J. Phys. Conf. Ser., vol. 2974, no. 1, p. 012030, Mar. 2025.

[43] S. Alven and B. A. Aderibigbe, “Chitosan-based scaffolds incorporated with silver nanoparticles for the treatment of infected wounds,” Pharmaceutics, vol. 16, 2024.